Effect of Specimen Size and Notch Root Radius on Dynamic Fracture Toughness of Heavy Wall Ductile Cast Iron

H. YAMAMOTO and T. KOBAYASHI
Department of Production Systems Engineering, Toyohashi University of Technology, 1–1 Hibarigaoka, Tempaku-cho, Toyohashi 440, Japan

ABSTRACT

Dynamic fracture toughness of heavy wall ductile cast iron for cask of spent nuclear fuel is evaluated mainly by the developed Computer Aided Instrumented Impact Testing (CAI) system. Moreover, effect of specimen size on J_d value is examined and it is shown that constant J_{Id} value is obtained by the specimen thickness of 20 mm (net specimen thickness: 16 mm) in side grooved Charpy type specimen. Effect of notch root radius ρ on the fracture toughness is also discussed and shown that the fracture toughness evaluated from the notched specimen with radius ρ follows the theoretical formula presented by Williams.

KEYWORDS

Dynamic fracture toughness; heavy wall ductile cast iron; cask; CAI system; size effect; notch root radius.

INTRODUCTION

Evaluation criteria of safety should be established for application of ductile cast iron to cask of spent nuclear fuel. However, the accident during transport must be assumed. It is insufficient to evaluate the fracture toughness only under static loading test. It is very important to evaluate dynamic fracture toughness (CRIEPI, 1987). One of the authors has already reported on the dynamic fracture of ductile cast iron since a past decade (for example; Kobayashi, 1979); and, in this study, critical evaluation of dynamic fracture toughness of the ductile cast iron for the cask is attempted.
The measurement of lower bound in the ductile-brittle transition curve of toughness is necessitated in the safety design for the cask. By the way, fracture toughness of iron or steel generally shows the temperature dependence. The present study is purposed to estimate reasonably the dynamic fracture toughness of ductile cast iron for the cask. Dynamic fracture toughness is evaluated by various test methods, including CAI (Computer

Aided Instrumented Impact Testing) system recently developed by Kobayashi et al. (Kobayashi et el., 1986, 1989).
Criterion on the validity of obtained dynamic value has not been established yet. The effect of specimen size on the validity is an important problem. It will be necessary to clarify whether small size specimen such as Charpy one used in this study offers valid dynamic elastic-plastic fracture toughness value J_{Id}. Also, in this study, the validity on the obtained dynamic J integral i.e. J_d values is examined and discussed.

By the way, for the practical use, the brittle fracture resistance of the cask must be finally evaluated on the basis of full-scale drop test at -40°C (a free drop through a distance of 9 m onto flat horizontal solid surface). It is general to introduce a fatigue crack in the fracture toughness test. However, such procedure is very difficult in the full-scale cask. Therefore, it will be important to develop the method to estimate the fracture toughness from the test of mechanically notched specimen. The effect of notch root radius on the fracture toughness is investigated from the above reason.

EXPERIMENTAL

Material and specimen geometries

Test material is a heavy wall ductile cast iron for cask (thickness: t=335 mm). It was fully ferritic annealed after casting. Table 1 gives the microstructual parameters where D_g is mean graphite diameter, d_g is mean free path of graphite, f_g is volume function of graphite, and D_f is mean ferrite grain diameter. All specimens were sectioned from 1/4t and 2/4t positions in the thickness direction.
The standard size (10x10x55 mm) V-notch Charpy specimen with a fatigue precrack was mainly used in the static and dynamic fracture toughness test. The specimens with various specimen thicknesses (B=W type; B= 10, 15, 20, 25 mm) and notch root radii (0(precrack), 0.05, 0.1, 0.15, 0.2, 0.25, 0.5, 1.0 mm) were used to study the effects of specimen size and notch root radius, respectively. In the case of the V type (notch root radius: 0.25 mm) side grooved specimen, the total depth of grooves was 20% of the gross section.

Table 1. Microstructural parameters of test material.

D_g (μm)	d_g (μm)	f_g (vol.%)	D_f (μm)
50.1	126.4	10.7	40.0

Test methods

The evaluation of static fracture toughness and J_R curve were carried out by the DC electrical potential method (EPM) under static loading condition (Kobayashi et al., 1988). Under the dynamic loading condition, the evaluation of dynamic fracture toughness J_d was made by the compliance changing rate method (CCM) as a rapid and inexpensive one to detect the crack initiation point (Kobayashi et al., 1986).
In the next, J_R curve was estimated from a single load-deflection curve using the key-curve method (Kobayashi et al., 1986). The effectiveness of these novel methods for evaluation of dynamic fracture toughness on ductile

cast iron has been already proved (Kobayashi et al., 1988). Tearing modulus (T_{mat}) was determined from a slope of the static and dynamic J_R curve.
In this study, in the linear elastic fracture temperature range, dynamic fracture toughness was evaluated by the impact response curve method (Kalthoff, 1985) with strain gage (gage length: 2 mm) attached near the tip of the precrack. This method is based on the concept that time variation of dynamic stress intensity factor K_I^{dyn} until fracture is same under the same impact condition. Namely, if the impact response curve is previously determined for the Young's modulus E and poisson's ratio ν identical specimen with a dull notch, dynamic fracture toughness can be obtained from the measured time-to-fracture (t_f).

In the dynamic fracture toughness test, the authors selected the impact velocity condition that satisfied the condition of E_0 (applied energy) $\geqq 3E_t$ (absorbed energy) presented by Kobayashi et al. (1987). As a result, in the case of dynamic fracture toughness test, impact velocity (V_0) was selected as 1.34 m/s. On the other hand, in the case of the specimen size effect test, impact velocity was 2.29 m/s.
The bending yield load (P_y) and the maximum load (P_m) were determined from a recorded load-deflection curve. The dynamic tensile yield stress (σ_{yd}) and the dynamic tensile strength (σ_{Bd}) were calculated by substituting P_y and P_m into the dynamic bending load P in the equation presented by Server (1979), and confirmed by Kobayashi (1984). The dynamic flow stress ($\sigma_{flow} = (\sigma_{yd} + \sigma_{Bd})/2$), which is used for judging the validity of the obtained fracture toughness values, was assumed in this way.

RESULT AND DISCUSSION

Evaluation of fracture toughness

Typical load-deflection curves recorded in the dynamic fracture toughness test at the various temperatures are shown in Fig.1. The fracture mode changed from the ductile to the brittle one with lowering of temperature.

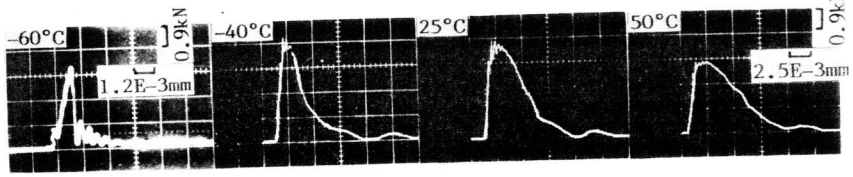

Fig.1 Typical load-deflection curves at various temperatures in the dynamic fracture toughness test (impact velocity: 1.34 m/s).

Figure 2 shows the plot of stress intensity factor K converted from J value by EPM and CCM under the static and dynamic loading conditions, respectively. J value in the transition temperature range was also measured

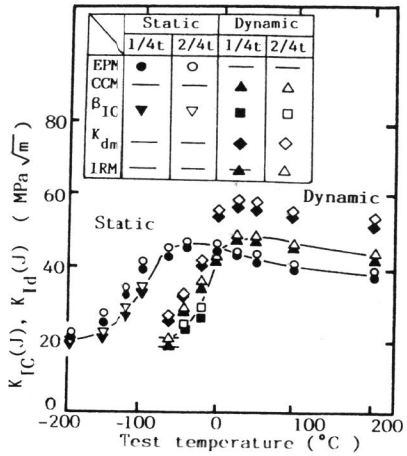

Fig.2 Transition curves of fracture toughness evaluated by various methods.

at the ductile crack initiation point. The J values satisfied the Eq.(1) of the valid condition of ASTM E813 at various test temperatures.

$$B,\ a_0 \geqq \alpha (J/\sigma_{flow}) \qquad (\alpha = 25) \qquad , \tag{1}$$

where B: specimen thickness, a_0: initial crack length, σ_{flow}: flow stress. In the figure, dynamic $K_{Id}(J)$ is smaller than static $K_{IC}(J)$ at lower temperature range. As a result, the fracture toughness of this material must be evaluated not by $K_{IC}(J)$ but $K_{Id}(J)$ below the room temperature. Furthermore, in this figure, K_{dm} value calculated from J integral obtained from the energy up to the maximum load is shown. This is the apparent fracture toughness, because the crack extension occurs generally prior to the maximum load. This figure shows that K_{dm} value largely overestimates the fracture toughness at higher temperature.
By the way, in recent years, the K value estimated from the J_{IC} test is not regarded as the K_{IC} in the transition region where brittle fracture is included. In this study, the estimation of fracture toughness in the transition region was made by β_{IC} method which has been presented by Irwin (1960). β_{IC} method is based on the plastic restriction dependence of the cleavage fracture, and the interrelation between K_{IC} and $K_{IC}(J)$ is defined as Eq.(2).

$$K_{IC}(J) = K_{IC} \sqrt{1 + 1.4(K_{IC}/\sigma_y)^4 / B^2} \tag{2}$$

This results estimated from β_{IC} method are shown with symbol β_{IC} in Fig.2. It is clear that β_{IC} method evaluates the lower bound of the static or dynamic fracture toughness in comparison with one obtained from conventional method.
Furthermore, it is clear from Fig.1 that the low stress brittle fracture occurs about -60°C. In this temperature range, oscillations due to inertial loading appear, therefore the impact response curve method has been applied. Dynamic fracture toughness K_{Id} determined from the impact response curve and the time-to-fracture is shown by symbol IRM in Fig.2. As a result, it is clearly found that the impact response curve method also evaluates the lower bound of dynamic fracture toughness in comparison with K_{dm} value.

Evaluation of tearing modulus (T_{mat})

Figure 3 shows temperature change of tearing modulus (T_{mat}) under the static and dynamic loading conditions. In this case, T_{mat} at Δa = 1 mm, which is estimated as the critical length of valid J controlled crack growth condition (Kobayashi et al., 1986) in this study, is used. Change of T_{mat} value shows a peak and it corresponds to the temperature where the maximum fracture toughness value is obtained. It is assumed that this behavior is caused by the decrease of ductile fracture at lower temperature range and the appearance of plastic collapse at higher temperature. However, T_{mat} generally shows the geometry dependence. Therefore, this result is one example and such study must be made more in the future.

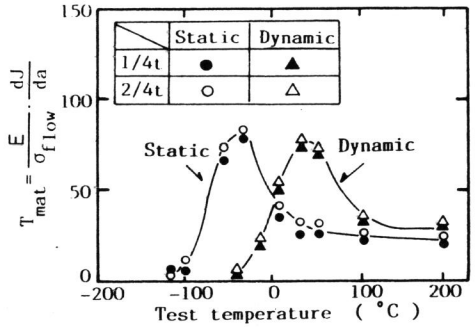

Fig.3 Temperature change of static and dynamic tearing modulus (T_{mat}).

Effect of the specimen size on elastic-plastic dynamic fracture toughness

The effect of the specimen size on J_d value is shown in Fig.4(a). The J_d value changes with the specimen thickness although the whole J_d values shown in Fig.4(a) satisfy the valid condition of Eq.(1) of ASTM E813. In the side grooved specimen, J_d value is constant above the specimen thickness (B) = 20

mm (net specimen thickness: B_{net} = 16 mm). On the other hand, J_d value of the ungrooved specimen does not become constant. Therefore, the size effect in the ungrooved specimen appears large.
However, since the valid condition for the specimen size in ASTM E813 is established under static loading, it is doubtful to apply this condition to dynamic loading.
The relationship between the specimen thickness B and J_d/σ_{flow} is shown in Fig.4(b). α in Eq.(1) is obtained by reading the reciprocal of gradient in the line which passes through the origin and the arrowed point from where J_d becomes constant in Fig.4(b). In result, α is about 243.0 for the side grooved specimen. Then, the valid condition under the dynamic loading is given by:

$$B \geqq 243.0\ (J_d/\sigma_{flow}) \quad . \tag{3}$$

It is clearly found that this result is ten times as large as valid condition of ASTM E813.

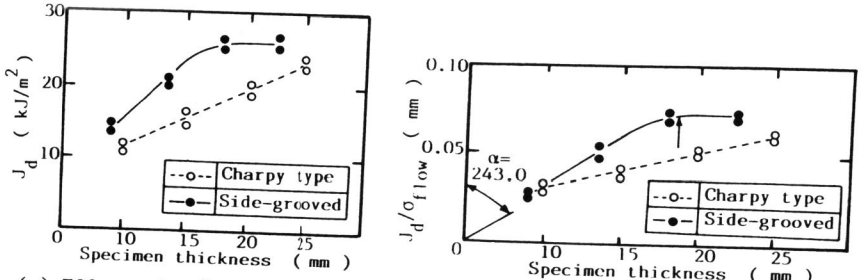

(a) Effect of specimen size on J_d value.

(b) Relation between specimen size and $J_d/$ flow.

Fig.4 Specimen size effect in cast iron.

By the way, a relation is assumed between the specimen size to obtain the valid J_{Id} value and the process zone size (ω_p) at the crack tip. The process zone size is about $\omega_p \simeq 2COD \simeq J_d/\sigma_{flow}$ from the elastic-plastic fracture mechanics's point of view (Rice et al., 1970). In other words, Eq.(1) requires the specimen thickness larger than 25 times as large as ω_p. From this point of view, it is expected that the valid condition for the specimen size under the dynamic loading condition is alleviated, because σ_{flow} increases under such condition. In fact, it has been reported by Shabbits et.al. (1969) that the valid condition is satisfied even in the size of 1/2.5 times thickness specimen in the dynamic test. However, the valid condition in this study appears severer. It may be related to a difference in the crack tip blunting angle between both processes (Kobayashi et al., 1989)

Effect of notch root radius on fracture toughness

Relationship between dynamic elastic strain energy release rate G_ρ converted from dynamic apparent fracture toughness J_ρ and notch root radius ρ at -40°C is shown in Fig.5. G_ρ is observed to increase with ρ .

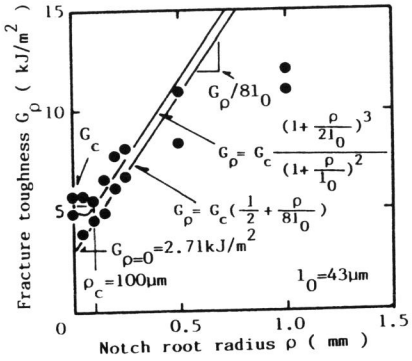

Fig.5 Effect of notch root radius on apparent dynamic fracture toughness at -40°C

By the way, the relation between critical elastic strain energy release rate G_c and notch root radius ρ has been represented by the following relation of Williams (1980). It has been confirmed that this relation establishes in the polymeric materials.

$$G_\rho = G_c \frac{(1+\rho/21_0)^3}{(1+\rho/1_0)^2} \tag{4}$$

where G_ρ : critical strain energy release rate in the specimen with notch root radius ρ , 1_0: characteristic distance. If $\rho \gg 1_0$, Eq.(4) will be given as follow.

$$G_\rho = G_c(\ 1/2 + \rho/81_0) \quad . \tag{5}$$

From this relation, it is assumed theoretically that a linear relation in the plot of G_ρ versus ρ is expected and its slope is $G_\rho/81_0$ and intersects the ordinate at $G_c/2$ level. $G_{\rho=0}$ obtained from extrapolation of the linear portion, G_ρ and estimated characteristic distance 1_0 are shown in Fig.5. The plot of G_ρ versus ρ is in a linear relation, and $G_{\rho=0}$ obtained from extrapolation of the linear portion is about a half of G_c obtained by precracked specimen.
On the other hand, the characteristic distance 1_0 equals to the ferrite grain diameter, and the critical notch root radius ρ_c agreed with the mean free path of graphite nodules. Moreover, if $G_\rho = G_c$ in Eq.(5), ρ_c is

theoretically given as $4l_0$. However, experimental result is $\rho_c=2.5l_0$. Relation between microstructure and fracture toughness must be investigated more in the future. However, it is found that the variation of the fracture toughness with the notch root radius follows the theoretical formula presented by Williams even in the ductile cast iron. And it is also suggested that the true fracture toughness can be estimated from the fracture toughness obtained from the notched specimen.

CONCLUSION

(1) Transition behaviour of the fracture toughness value and J_R curve have been reasonably evaluated by CAI system.
(2) It has been clarified that β_{IC} method by Irwin evaluates the lower bound of fracture toughness which is necessary for the safety design in the transition temperature region.
(3) It has been shown that the dynamic fracture toughness in the low stress brittle fracture at lower temperature range is effectively evaluated by the impact response curve method.
(4) It has been shown that T_{mat} value has decreased at lower and higher temperature range. This result may be due to the decrease of ductile fracture at lower temperature range and the plastic collapse at higher temperature one.
(5) It is found that constant dynamic elastic-plastic fracture toughness is obtained with the specimen thickness of 20 mm (net specimen thickness 16 mm) in the side grooved Charpy type specimen. The valid condition for the specimen size determined under dynamic loading condition appears severer than that of ASTM E813.
(6) It has been shown that the variation of the dynamic fracture toughness with notch root radius follows the theoretical formula presented by Williams.

REFERENCE

Central Research Institute of Electric Power Industry (CRIEPI) (1987). Report of Ductile Cast Iron Cask QTA Committee. CRIEPI, Japan.
Irwin, G.R. (1960). J. bas. Engng., 6, 417.
Kalthoff, J.K. (1985). Int. J. Fract., 27, 227.
Kobayashi, T. (1979). Trans. ISIJ, 19, 676.
Kobayashi, T. (1984). Engng. Fract. Mech., 19, 67.
Kobayashi, T., I. Yamamoto and M. Niinomi (1986). Engng. Fract. Mech., 24, 773.
Kobayashi, T., I. Yamamoto and M. Niinomi (1987). Engng. Fract. Mech., 26, 83.
Kobayashi, T. and H. Yamamoto (1988). Met. Trans., 19A, 379.
Kobayashi, T., T. Kazino, M. Kamimura and H. Ikawa (1989). Proc. ICF7, to appear.
Rice, J. R. and M. J. Johnson (1970). Inelastic Behavior of Solids, 641, McGraw-Hill, New York.
Server, W. L. (1979). ASTM STP 668, 493.
Shabbits, W. O., W. H. Pryle and E. T. Wessel (1969). Steel Technology Program Technical Report, No.6, Westinghouse Electric Corp., Pittsburgh.
Williams, J. G. (1980). Metal Science, Aug.-Sept., 334.